

Supporting Information

ARYLAZOIMIDAZOLES REVAMPED BY QUARTERNIZATION OR DIMERIZATION; ANOTHER GAIN IN FUNCTIONALITY OF AN INDUSTRIAL DYESTUFF FAMILY BY TASK-SPECIFIC SIDE-CHAIN SUBSTITUENTS

Sandro Neuner,¹ Christoph Kreutz,² Thomas Müller,² Paul Mayer,³ Günther Bonn,³ Thomas Ibrich,⁴ Ulrich J. Griesser,⁴ Klaus Wurst,¹ Volker Kahlenberg,⁵ Sven Nerdinger,^{6*} and Herwig Schottenberger ^{1*}

¹⁻⁵Leopold Franzens University, 6020 Innsbruck, Austria; ¹Institute of General, Theoretical & Inorganic Chemistry, Innrain 80-82; ²Institute of Organic Chemistry, Innrain 80-82; ³Institute of Analytical Chemistry, Innrain 80-82; ⁴Institute of Pharmacy, Innrain 52c; ⁵Institute of Mineralogy & Petrography, Innrain 52; ⁶Sandoz GmbH, Biochemiestr. 10, 6250 Kundl, Austria.

E-mail: sven.nerdinger@sandoz.com; herwig.schottenberger@uibk.ac.at

Table of Contents

Crystal Structures and PRXD Data	3
¹ H-NMR, ¹³ C-NMR, ¹⁹ F-NMR, IR-absorption and UV/VIS spectra.....	6
1,3-Dibenzyl-2-((4-fluorophenyl)diazenyl)-1H-imidazolium bromide (1)	6
2-((4-Fluorophenyl)diazenyl)-1,3-bis-(4-vinylbenzyl)-1H-imidazolium hexafluorophosphate (2)	7
2-((4-Fluorophenyl)diazenyl)-1,3-bis(2-oxo-2-phenylethyl)-1H-imidazolium hexafluorophosphate (3)	8
3,3'-(2-((4-Fluorophenyl)diazenyl)-1H-imidazolium-1,3-diyl)bis(propane-1-sulfonate) potassium salt (4)	9
1,3-Diethyl-2-((4-fluorophenyl)diazenyl)-1H-imidazolium tetrafluoroborate (5)	11
2-((4-Fluorophenyl)diazenyl)- 1,3-bis-(propargyl)-1H-imidazolium hexafluorophosphate (6).....	15
1,3-Bis(2-((4-fluorophenyl)diazenyl)-1H-imidazol-1-yl)propan-2-ol (7)	16
Hot stage microscopy – contact preparation of compound (5).....	18
Dichroism of 2-(4-fluorophenyl)diazenyl)-1,3-diethylimidazolium tetrafluoroborate (5).....	20

Crystal Structures and PRXD Data

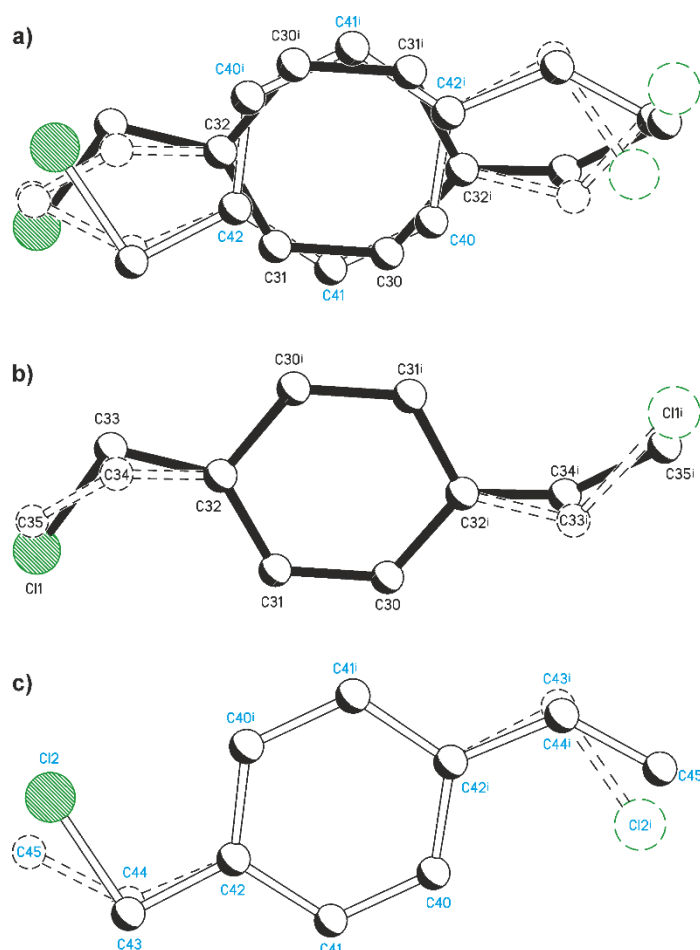
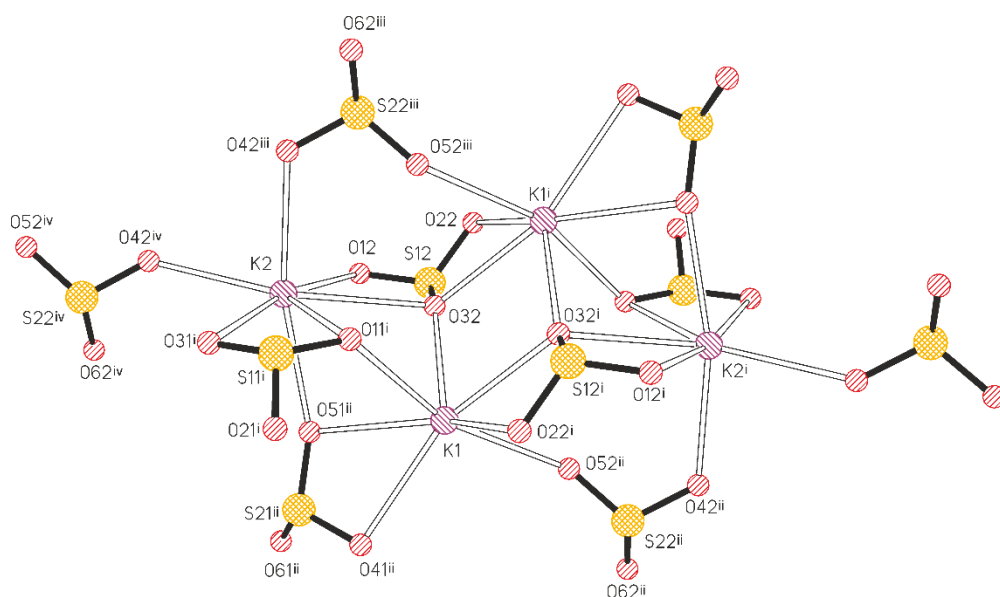


Figure S1. Disorder of the VBzCl molecule in $2 \cdot 0.5$ 4-VBzCl over an inversion centre. **a)** Overlay of all four disorder fragments. The same view, but showing only two inversion-related disorder components: **b)** two symmetry-related components having a relative occupancy of 30% each and **c)** two symmetry-related components having a 20% occupancy each. Symmetry operation (i) $-x, -y, 1-z$ (H atoms omitted for clarity).



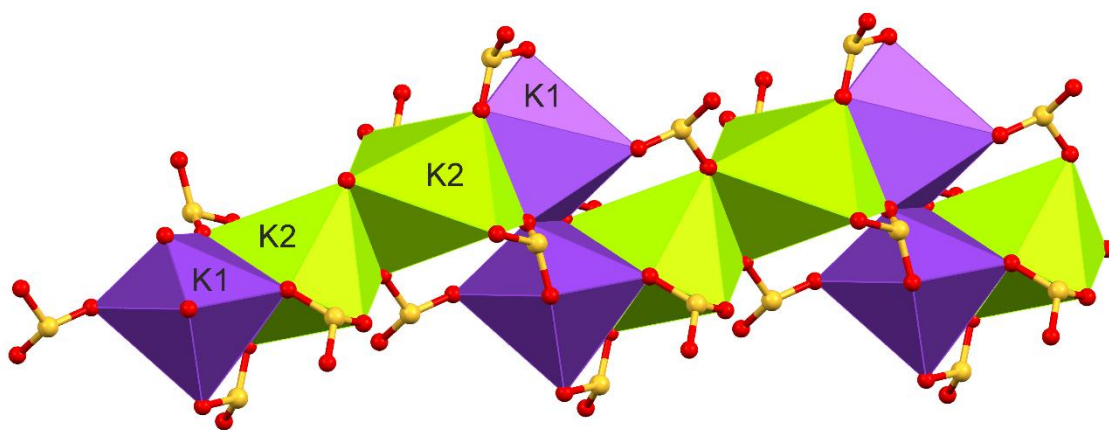


Figure S2. Crystal structure of compound **4**. **Top:** seven-fold coordination of K1 and K2 by sulfonate-O atoms belonging to five different sulfonate groups. Symmetry operations (i) $-x - 1, -y - 1, -z$ (ii) $-x - 1, -y, -z$ (iii) $-x, -y - 1, -z$ (iv) $-x, -y, -z$. **Bottom:** Chain of coordination polyhedra of K1 (purple) and K2 (green) which are connected either *via* a common edge (K1/K1 and K2/K2) or face (K1/K2).

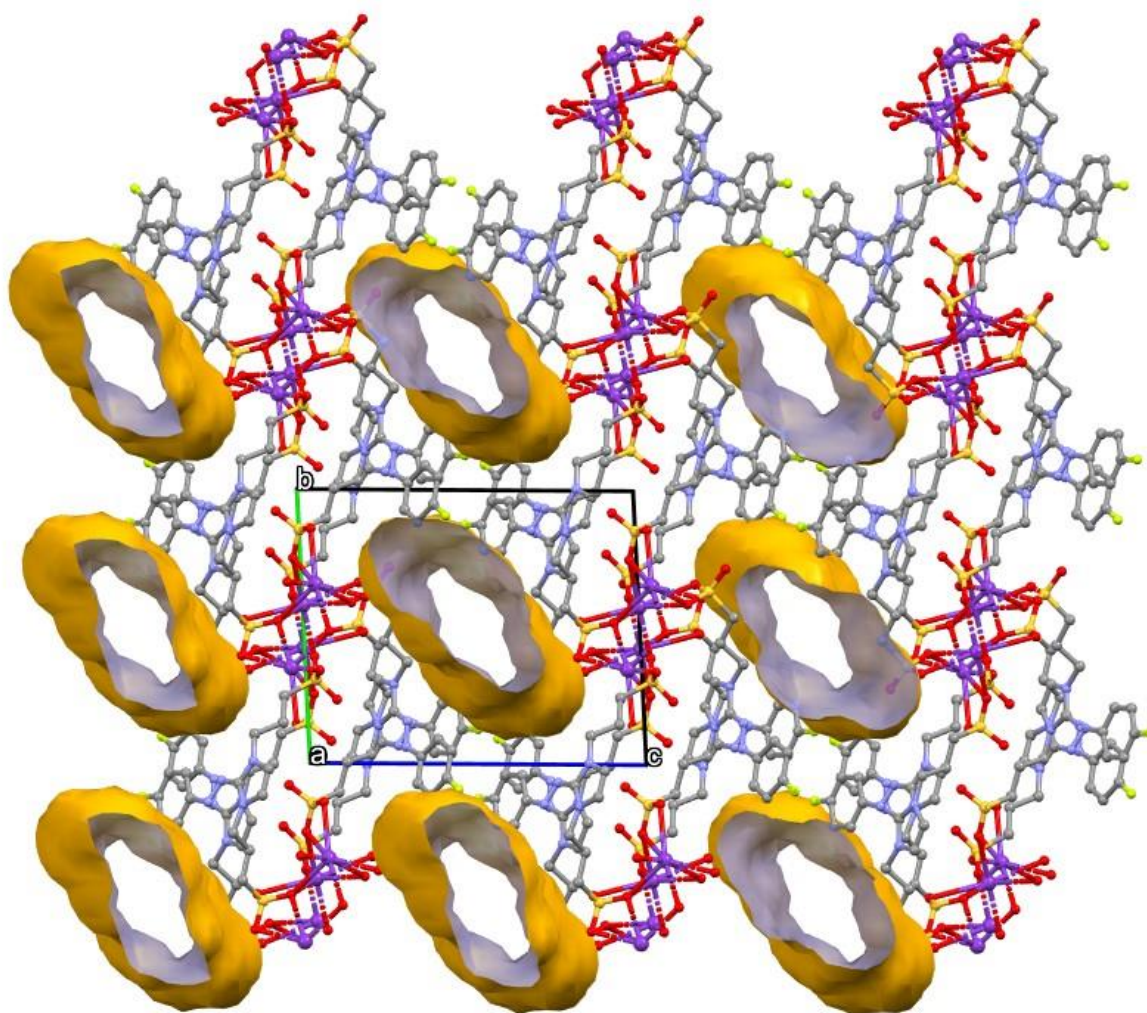


Figure S3. Crystal structure of **4S**, viewed along $[100]$, showing the 3D framework of anions connected by KO_7 coordination polyhedral. This framework contains empty channels (yellow shapes) which offer a solvent accessible volume of 500.9 \AA^3 per unit cell (250 \AA^3 or per formula unit) and are occupied by disordered solvent molecules. The data were not sufficient to accurately determine positions of disordered solvent molecules (assumed to be EtOH). The presence of 132 electrons per unit cell (or 66 per formula unit) in these channels was indicated by an analysis with the *Platon/Squeeze* software (A. Spek. *Acta Cryst.*, 2015, **C71**, 9.)

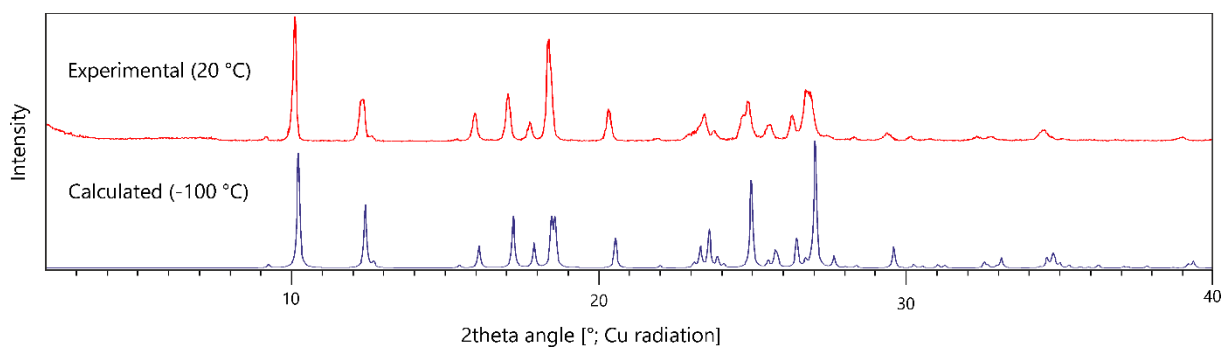


Figure S4. Experimental powder X-ray pattern for compound **4**, recorded at room temperature (top) and calculated based on the single-crystal structure data of **4**.

Table S1. Hydrogen bonds [\AA and $^\circ$] for **7** · **0.5 H₂O**.

$D-H\cdots A$	d_{D-H}	$d_{H\cdots A}$	$d_{D\cdots A}$	$\angle(DHA)$
O(7)—H(7)···N(15)	0.84	1.99	2.830(5)	178.4
O(14)—H(14)···N(18)	0.84	1.87	2.714(5)	178.5
O(56)—H(56A)···N(13)	0.83	2.05	2.839(6)	159.8
O(56)—H(56B)···O(14)#1	0.86	2.48	2.908(6)	111.9

Symmetry transformations used to generate equivalent atoms:

#1 $x+1, y-1, z$

$^1\text{H-NMR}$, $^{13}\text{C-NMR}$, $^{19}\text{F-NMR}$, IR-absorption and UV/VIS spectra

1,3-Dibenzyl-2-((4-fluorophenyl)diazenyl)-1H-imidazolium bromide (1)

$^1\text{H NMR}$ (300 MHz, $\text{DMSO-}d_6$) δ = 8.13 (m, 2H), 7.54 (m, 2H), 7.39 (m, 12H), 5.80 (s, 4H) ppm.

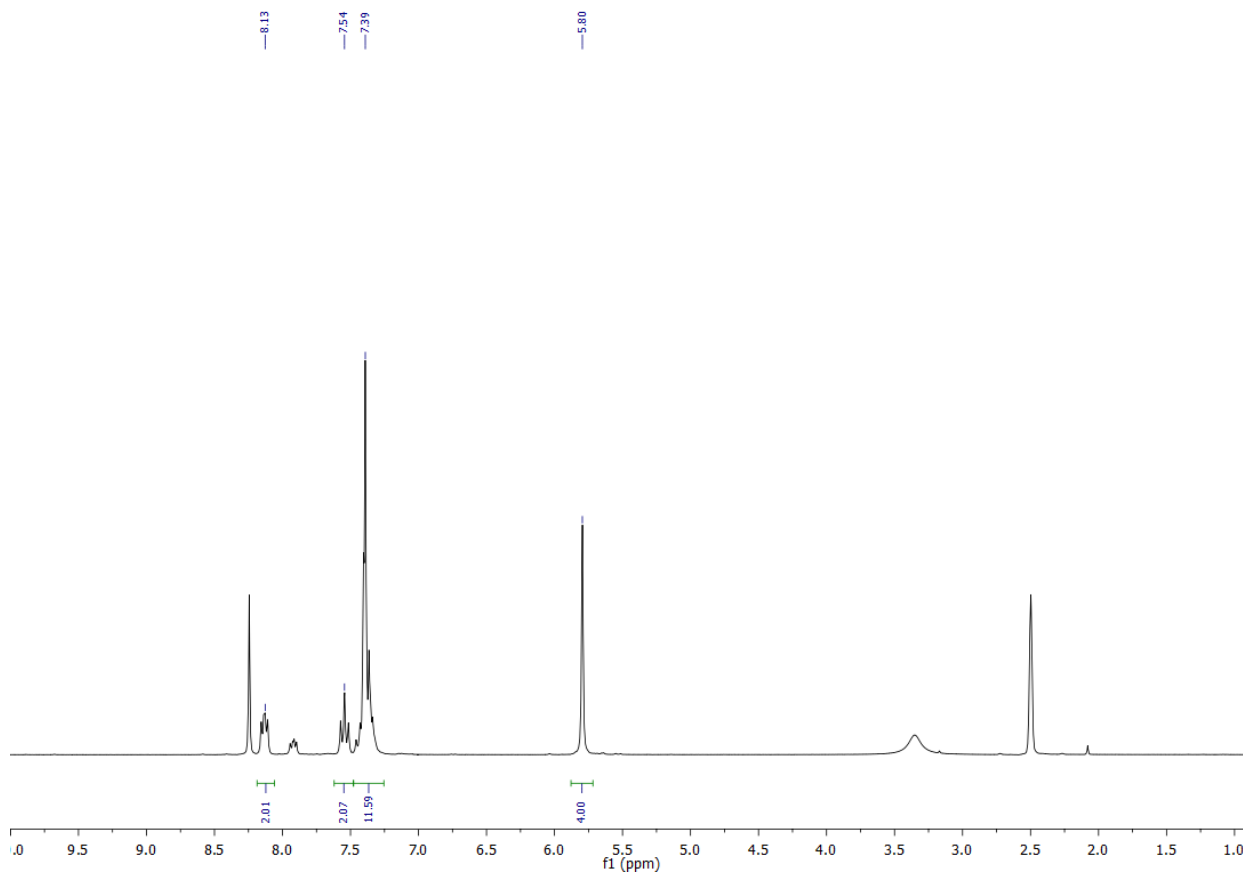


Figure S5. $^1\text{H-NMR}$ ($\text{DMSO-}d_6$) of 1,3-Dibenzyl-2-((4-fluorophenyl)diazenyl)-1H-imidazolium bromide (1).

**2-((4-Fluorophenyl)diazenyl)-1,3-bis-(4-vinylbenzyl)-1H-imidazolium
hexafluorophosphate (2)**

$^1\text{H NMR}$ (300 MHz, $\text{DMSO-}d_6$) δ = 7.97 (m, 2H), 7.49 (m, 12H), 6.78 – 6.65 (m, 2H), 5.86 – 5.72 (m, 6H), 5.29-5.23 (m, 2H) ppm.

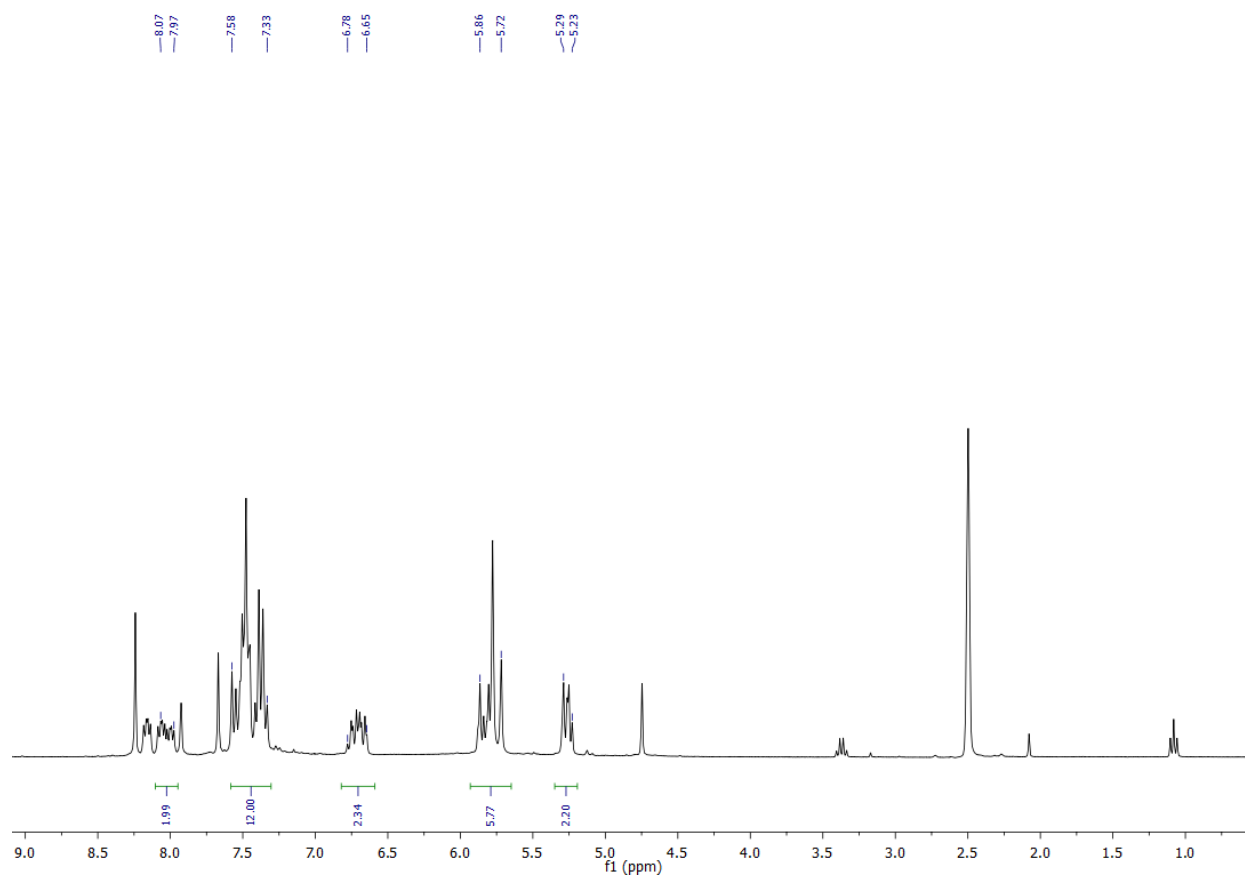


Figure S6. $^1\text{H-NMR}$ ($\text{DMSO-}d_6$) of 2-((4-Fluorophenyl)diazenyl)-1,3-bis-(4-vinylbenzyl)-1H-imidazolium hexafluorophosphate (**2**). The spectrum is compromised due to inclusion of 4-vinylbenzyl chloride into the crystal lattice.

2-((4-Fluorophenyl)diazenyl)-1,3-bis(2-oxo-2-phenylethyl)-1H-imidazolium hexafluorophosphate (3)

$^1\text{H NMR}$ (300 MHz, $\text{DMSO-}d_6$) δ = 8.15 (s, 2H), 8.13 (s, 2H), 8.11 (s, 2H), 7.83 (t, J = 7.4 Hz, 2H), 7.69 (t, J = 7.9 Hz, 5H), 7.66 – 7.63 (m, 2H), 7.39 (t, J = 8.8 Hz, 2H), 6.46 (s, 4H) ppm.

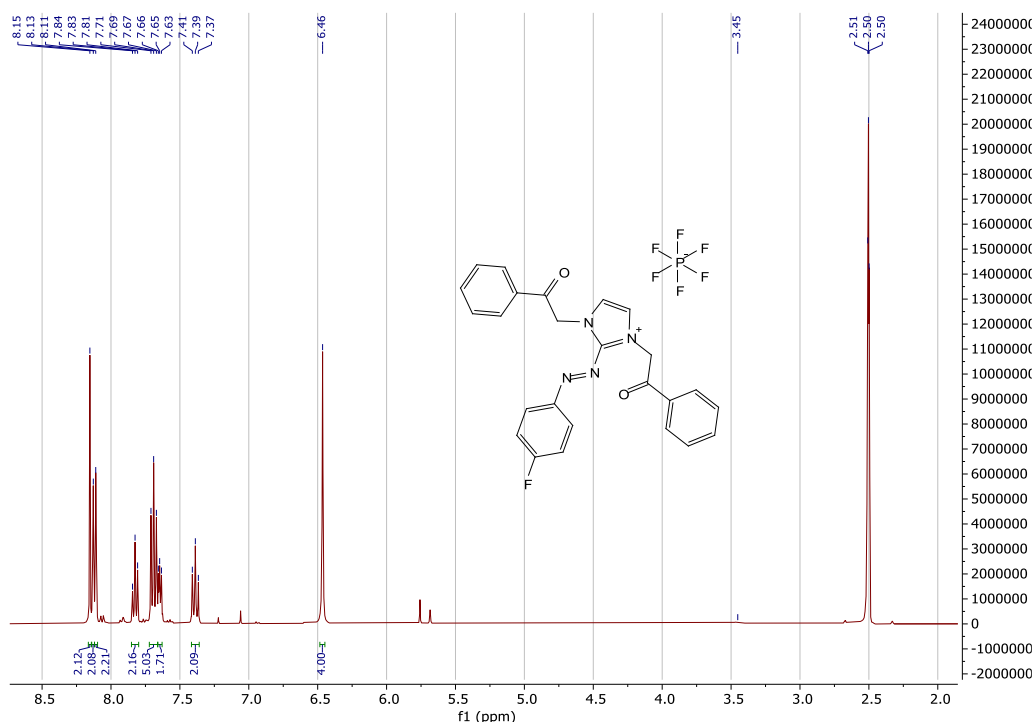


Figure S7. $^1\text{H-NMR}$ ($\text{DMSO-}d_6$) of 2-((4-Fluorophenyl)diazenyl)-1,3-bis(2-oxo-2-phenylethyl)-1H-imidazolium hexafluorophosphate (3)

IR(neat): ν = 3179 (w), 3069 (w), 3013 (w), 2963 (w), 1692 (m), 1596 (m), 1465 (m), 1354 (m), 1305 (m), 1235 (m), 1141 (m), 1078 (w), 1002 (w), 825 (s), 754 (m), 686 (m) cm^{-1} .

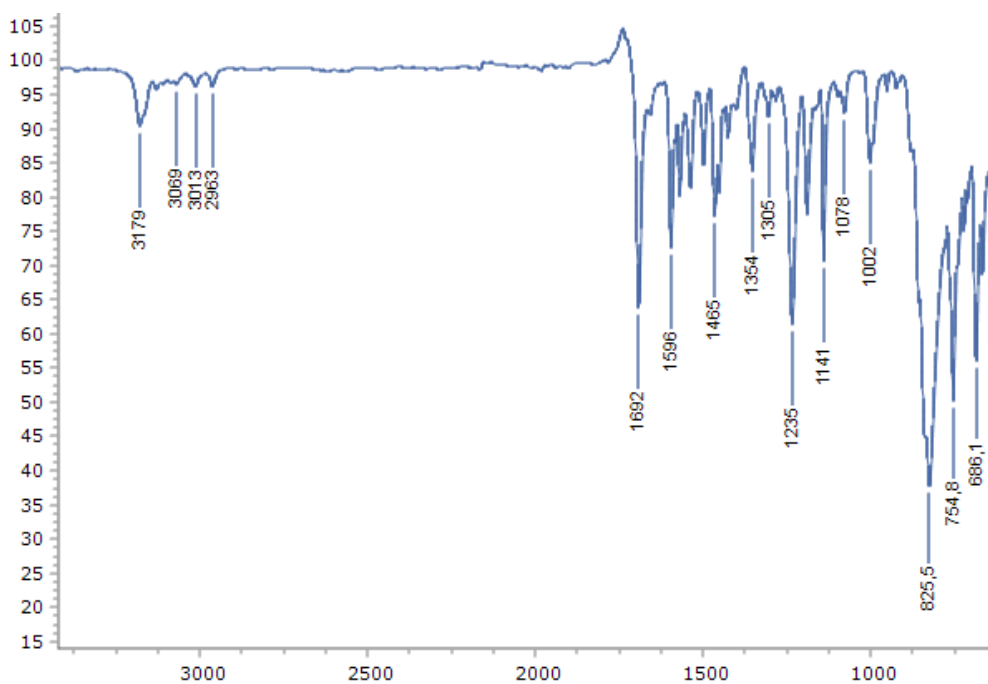


Figure S8. IR- absorption spectra (neat) of 2-((4-Fluorophenyl)diazenyl)-1,3-bis(2-oxo-2-phenylethyl)-1H-imidazolium hexafluorophosphate (3)

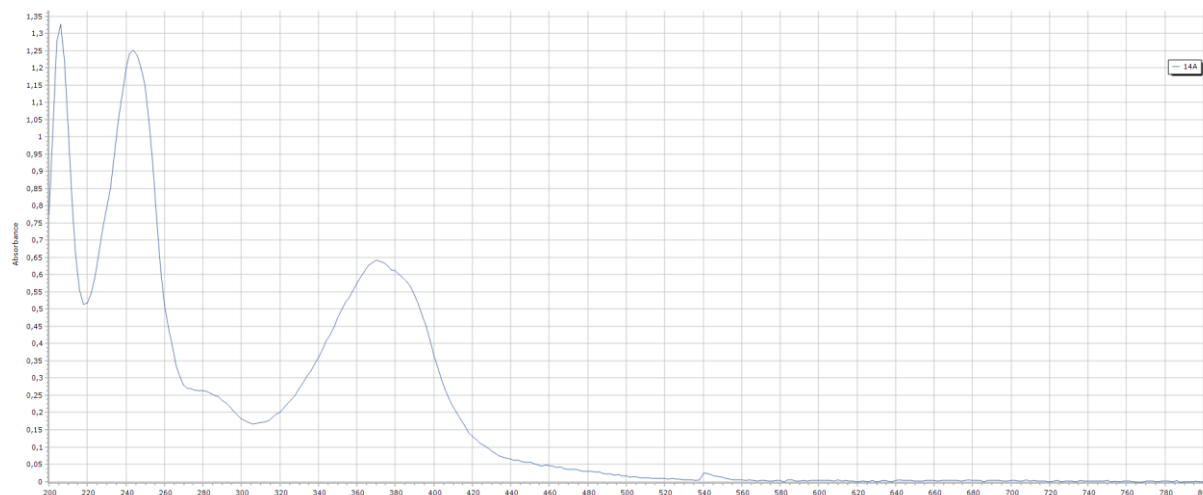


Figure S9. UV/Vis spectra (neat) of 2-((4-Fluorophenyl)diazenyl)-1,3-bis(2-oxo-2-phenylethyl)-1H-imidazolium hexafluorophosphate (**3**)

3,3'-(2-((4-Fluorophenyl)diazenyl)-1H-imidazolium-1,3-diyl)bis(propane-1-sulfonate) potassium salt (4**)**

^1H NMR (300 MHz, $\text{DMSO-}d_6$) δ = 8.37 (s, 2H), 8.11 (s, 2H), 7.54 (s, 2H), 4.62 (s, 4H), 3.46 (s, 4H), 2.15 (s, 4H) ppm.

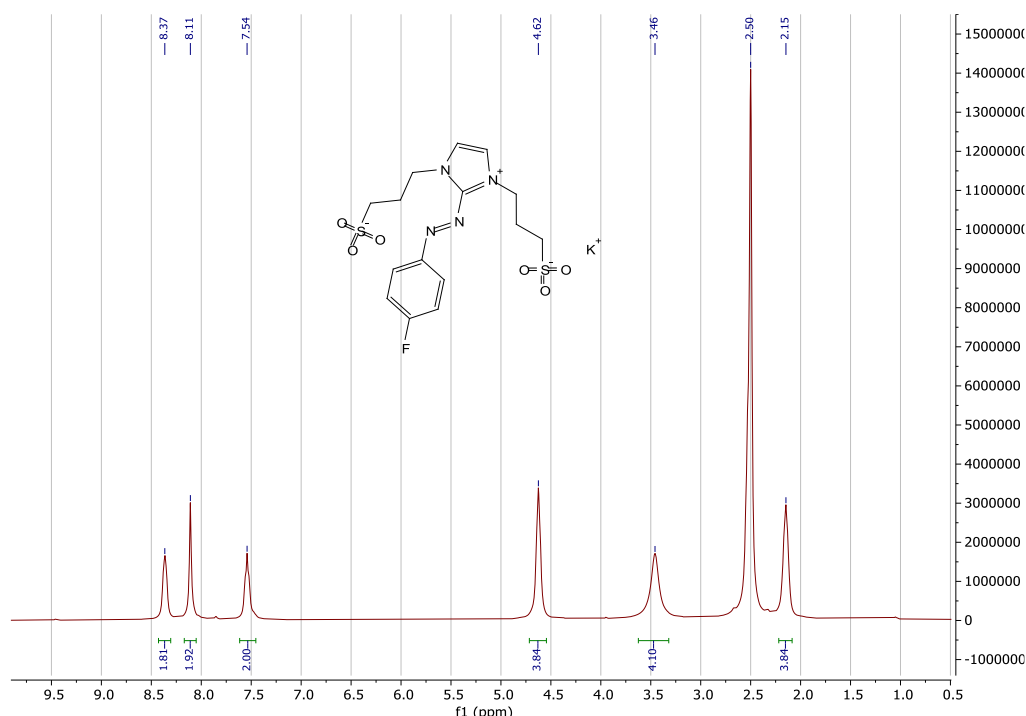


Figure S10. ^1H -NMR ($\text{DMSO-}d_6$) of 3,3'-(2-((4-Fluorophenyl)diazenyl)-1H-imidazolium-1,3-diyl)bis(propane-1-sulfonate) potassium salt (**4**)

IR(neat): ν = 3437 (w), 3103 (w), 2977 (w), 2630 (w), 2539 (w), 1590 (m), 1460 (m), 1309 (w), 1172 (s), 1034 (s), 856 (m), 802 (w), 733 (w), cm^{-1} .

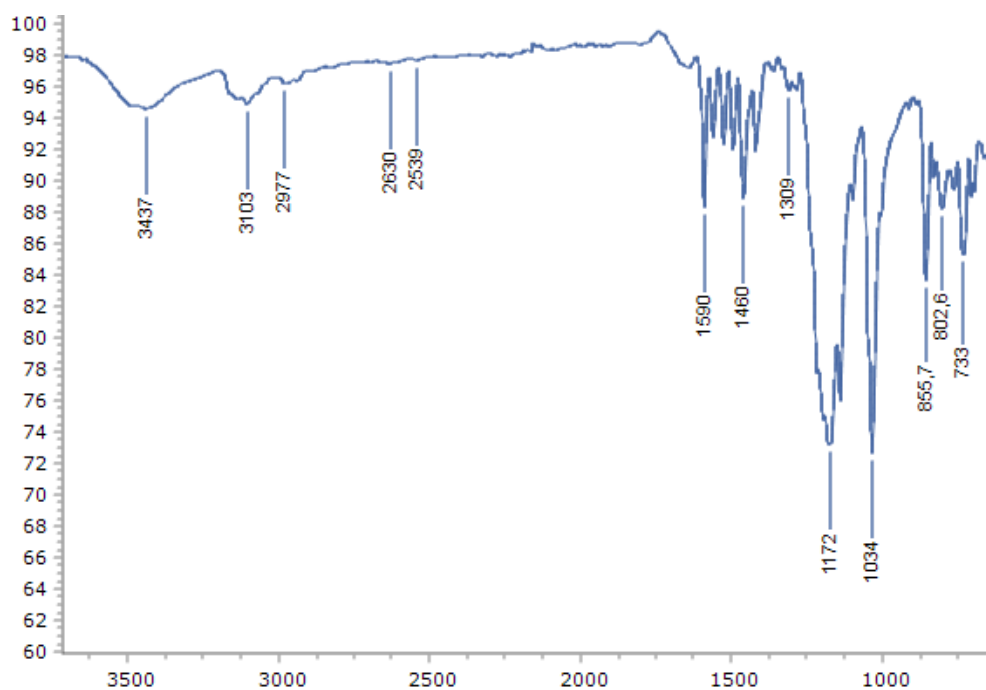


Figure S11. IR- absorption spectra (neat) of 3,3'-(2-((4-Fluorophenyl)diazenyl)-1H-imidazolium-1,3-diyl)bis(propane-1-sulfonate) potassium salt (**4**)

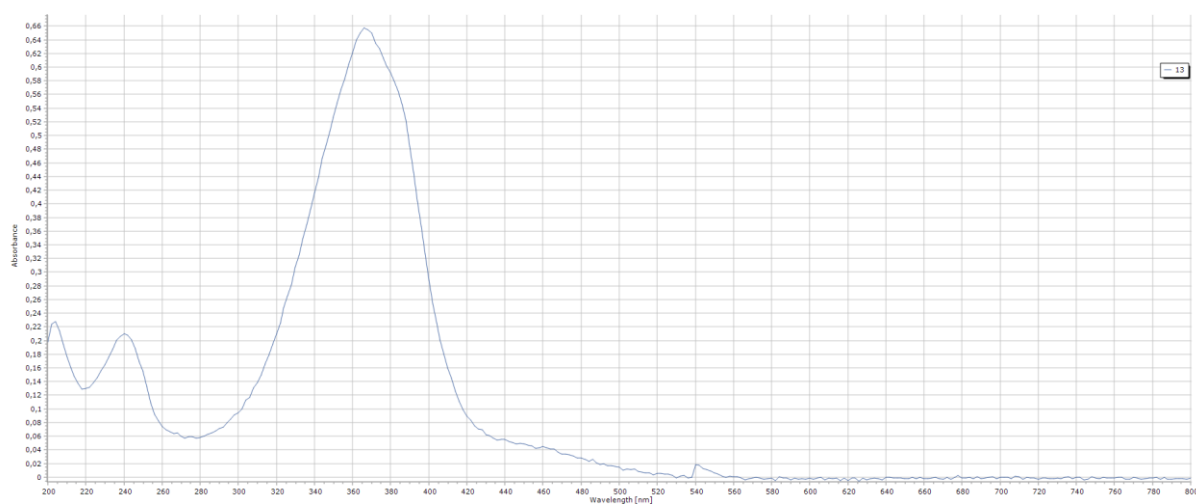


Figure S12. UV/Vis spectra (neat) of 3,3'-(2-((4-Fluorophenyl)diazenyl)-1H-imidazolium-1,3-diyl)bis(propane-1-sulfonate) potassium salt (**4**)

1,3-Diethyl-2-((4-fluorophenyl)diazenyl)-1H-imidazolium tetrafluoroborate (5)

^1H NMR (300 MHz, $\text{DMSO-}d_6$) δ = 8.15 (m, 4H), 7.56 (m, 2H), 4.54 (m, 4H), 1.47 (s, 6H) ppm.

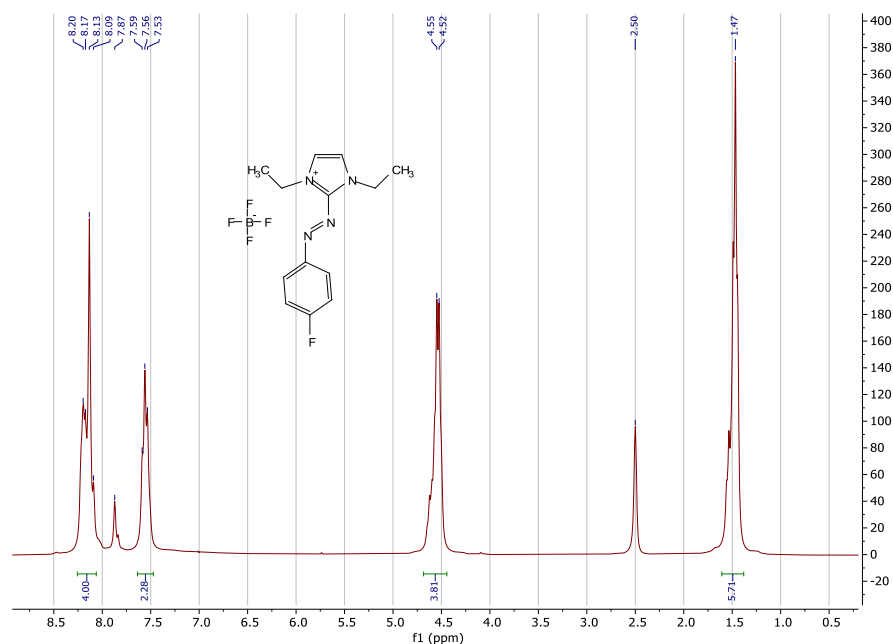


Figure S13. ^1H -NMR ($\text{DMSO-}d_6$) of 1,3-Diethyl-2-((4-fluorophenyl)diazenyl)-1H-imidazolium tetrafluoroborate (5)

^{13}C NMR (176 MHz, $\text{CH}_2\text{Cl}_2\text{-}d_2$) δ = 168.63, 168.54, 167.15, 167.06, 149.77, 149.17, 146.71, 142.92, 128.21, 128.15, 127.46, 127.40, 124.12, 123.28, 121.34, 121.17, 117.82, 117.69, 117.55, 117.37, 46.26, 43.96, 16.06, 15.69 ppm; multiple signals, attributed to equilibrium of isomers.

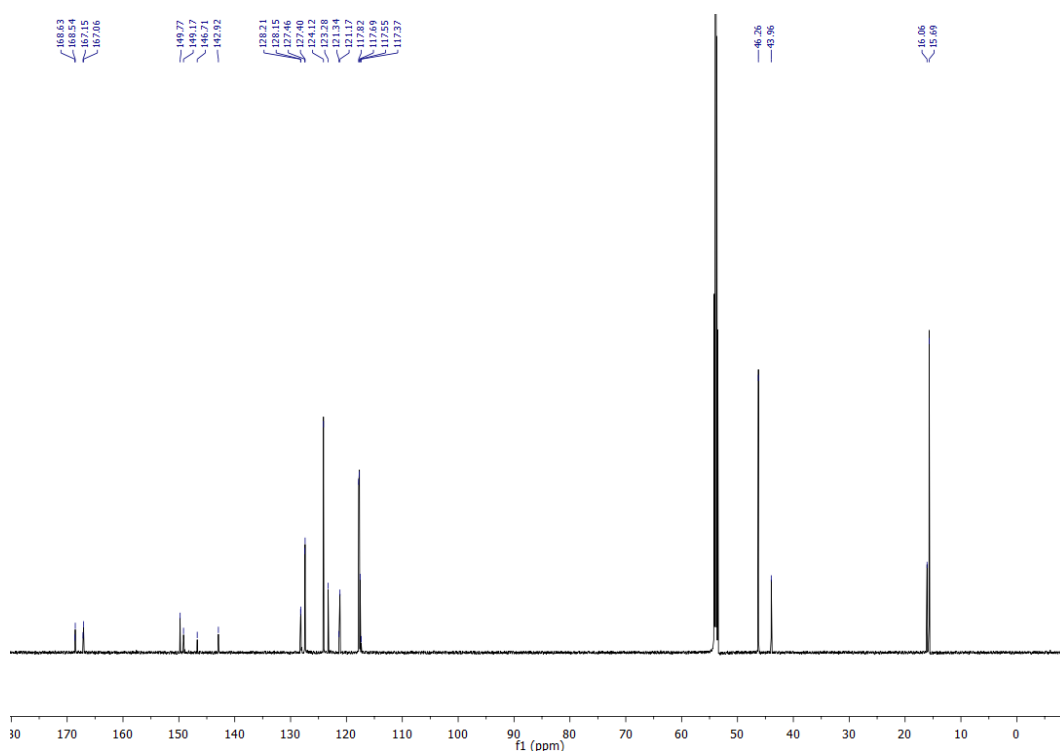


Figure S14. ^{13}C -NMR ($\text{CH}_2\text{Cl}_2\text{-}d_2$) of 1,3-Diethyl-2-((4-fluorophenyl)diazenyl)-1H-imidazolium tetrafluoroborate (5)

^{19}F NMR (659 MHz, $\text{CH}_2\text{Cl}_2\text{-}d_2$) δ = -100.33, -151.86 ppm.

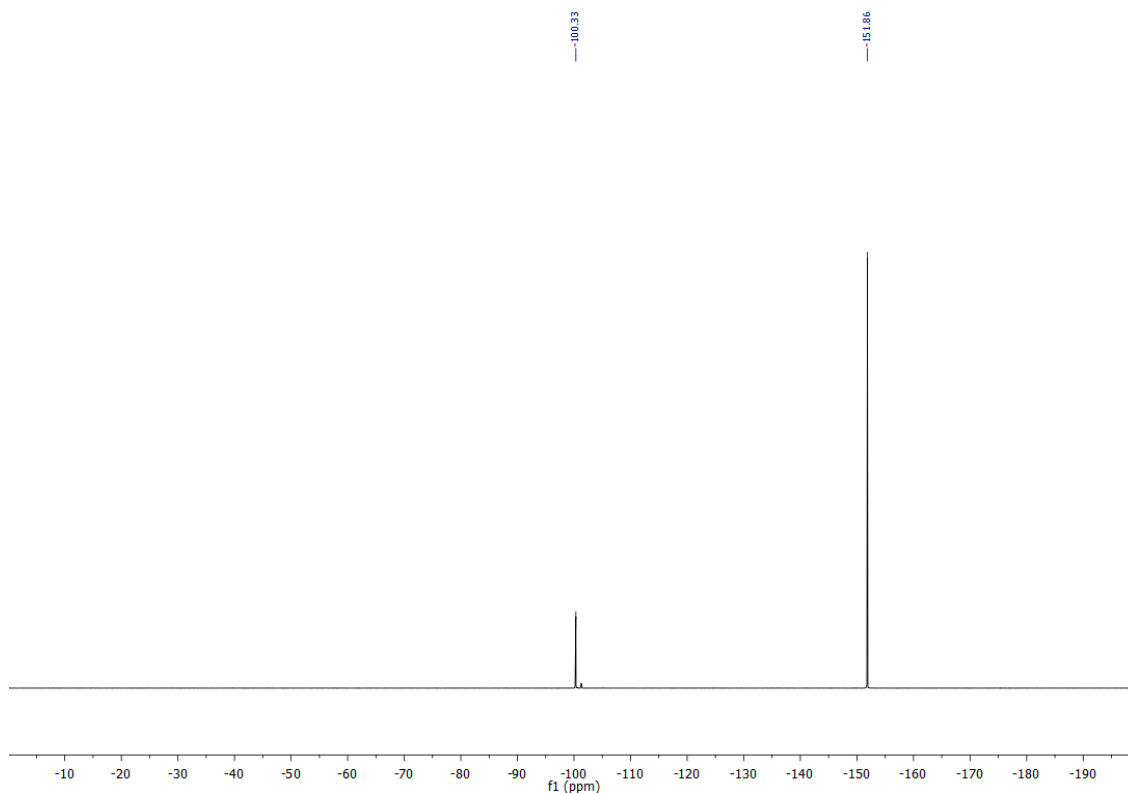
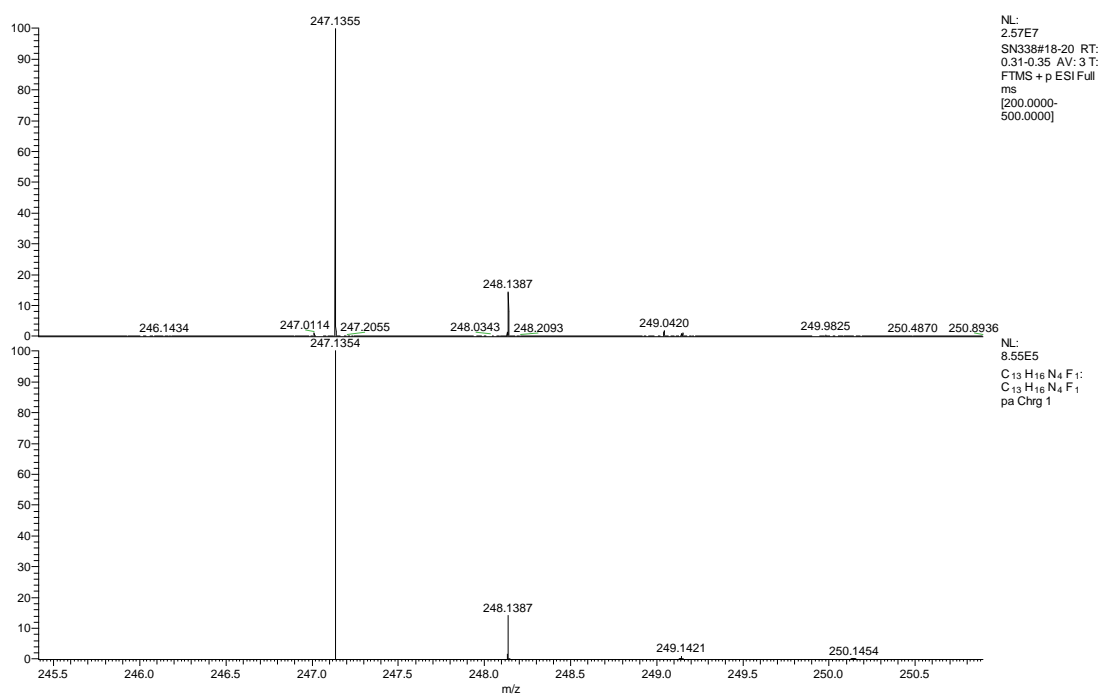


Figure S15. ^{19}F -NMR ($\text{CH}_2\text{Cl}_2\text{-}d_2$) of 1,3-Diethyl-2-((4-fluorophenyl)diazenyl)-1H-imidazolium tetrafluoroborate (5)



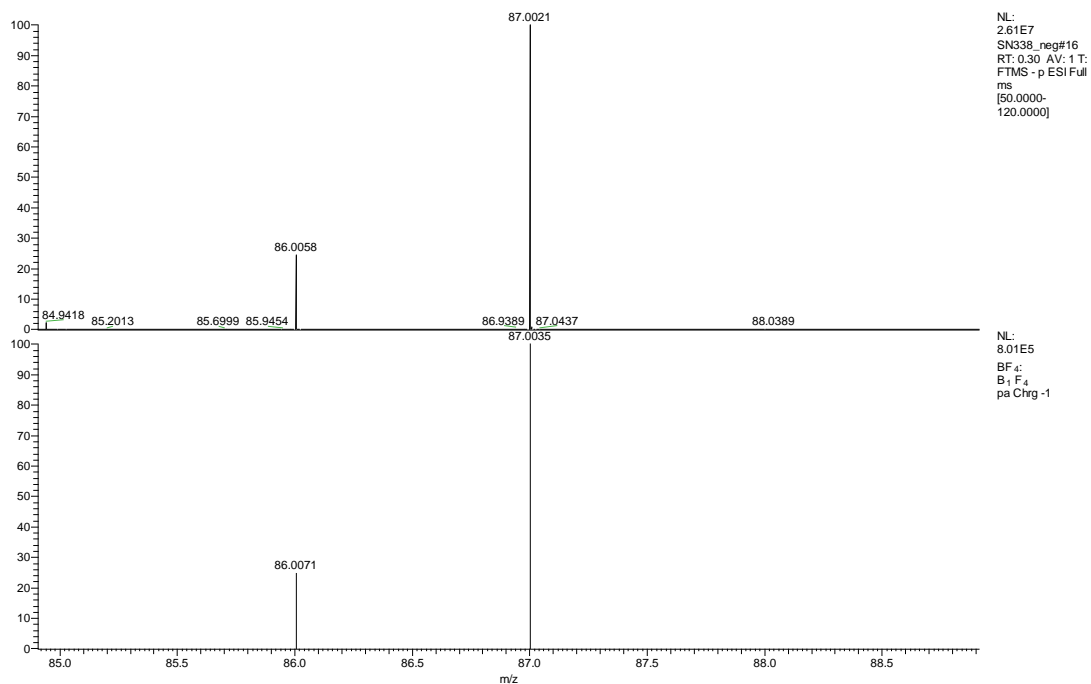


Figure S16. HRMS of 1,3-Diethyl-2-((4-fluorophenyl)diazenyl)-1H-imidazolium tetrafluoroborate (**5**)

IR(neat): ν = 3590 (w), 3144 (w), 2994 (w), 1589 (m), 1524 (m), 1482 (m), 1292 (w), 1229 (m), 1145 (m), 1032 (s), 856 (m), 780 (m), 703(m) cm^{-1} .

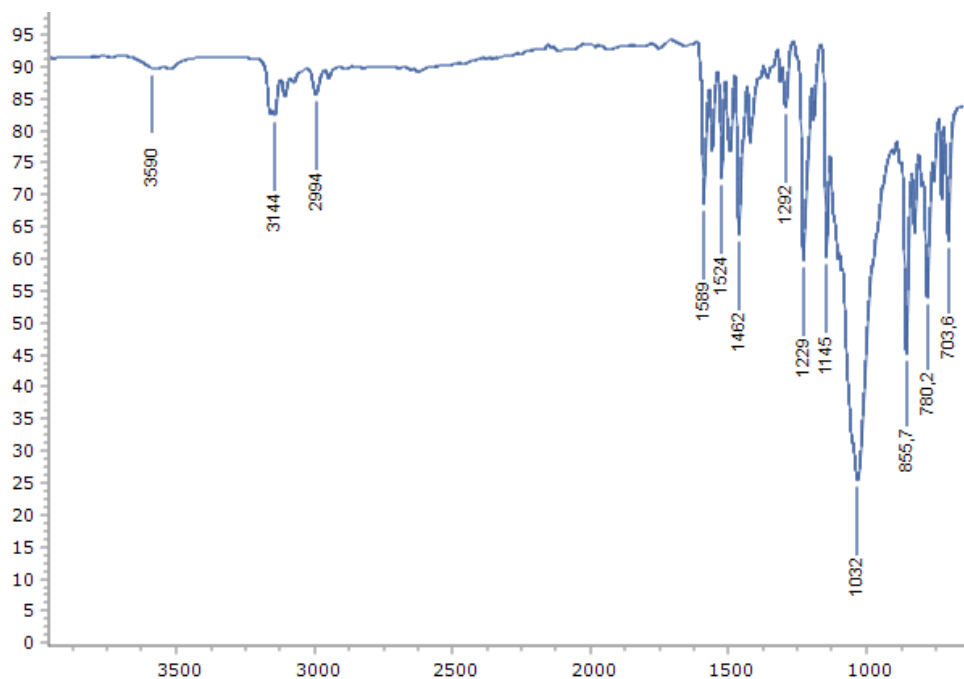


Figure S17. IR- absorption spectra (neat) of 1,3-Diethyl-2-((4-fluorophenyl)diazenyl)-1H-imidazolium tetrafluoroborate (**5**)

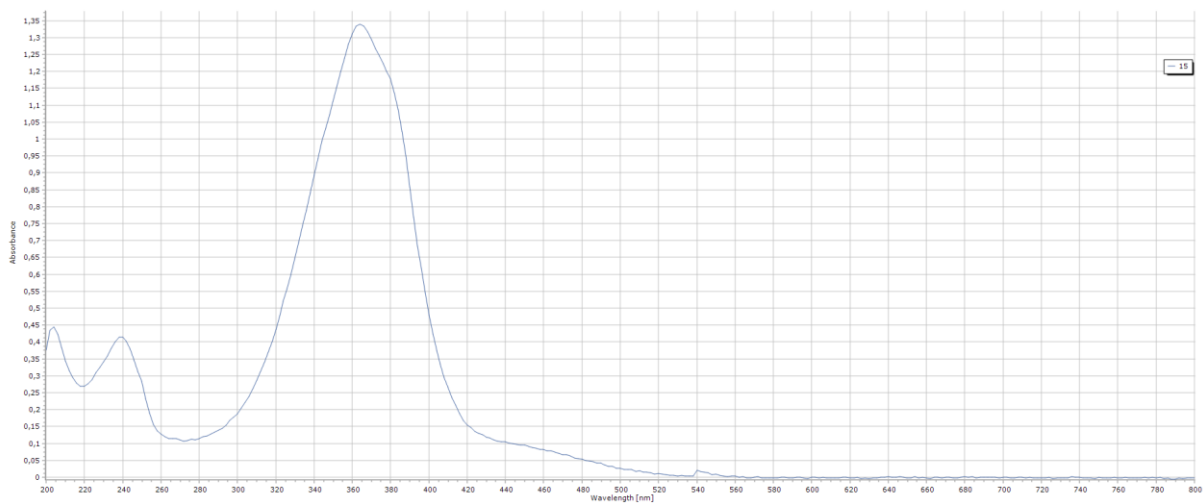


Figure S18. UV/Vis spectrum of 1,3-Diethyl-2-((4-fluorophenyl)diazenyl)-1H-imidazolium tetrafluoroborate (**5**)

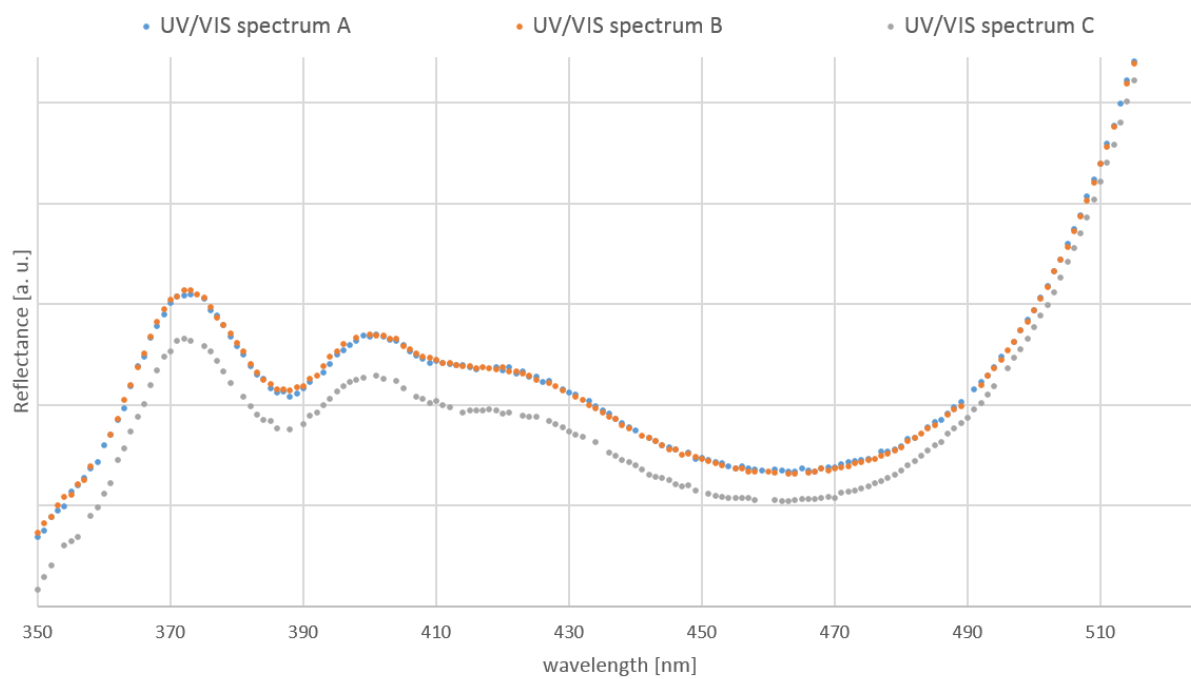


Figure S19. UV/Vis Reflectance spectra of 1,3-Diethyl-2-((4-fluorophenyl)diazenyl)-1H-imidazolium tetrafluoroborate (**5**). Spectra B and C correspond to reflectance spectra after irradiation with LED light of 365 nm and 535 nm for five minutes, respectively.

**2-((4-Fluorophenyl)diazenyl)- 1,3-bis-(propargyl)-1H-imidazolium
hexafluorophosphate (6)**

^1H NMR (300 MHz, $\text{DMSO-}d_6$) δ = 8.21 (s, 2H), 7.59 (m, 2H), 7.30 (m, 2H), 5.49 (m, 4H), 3.80 (m, 2H) ppm.

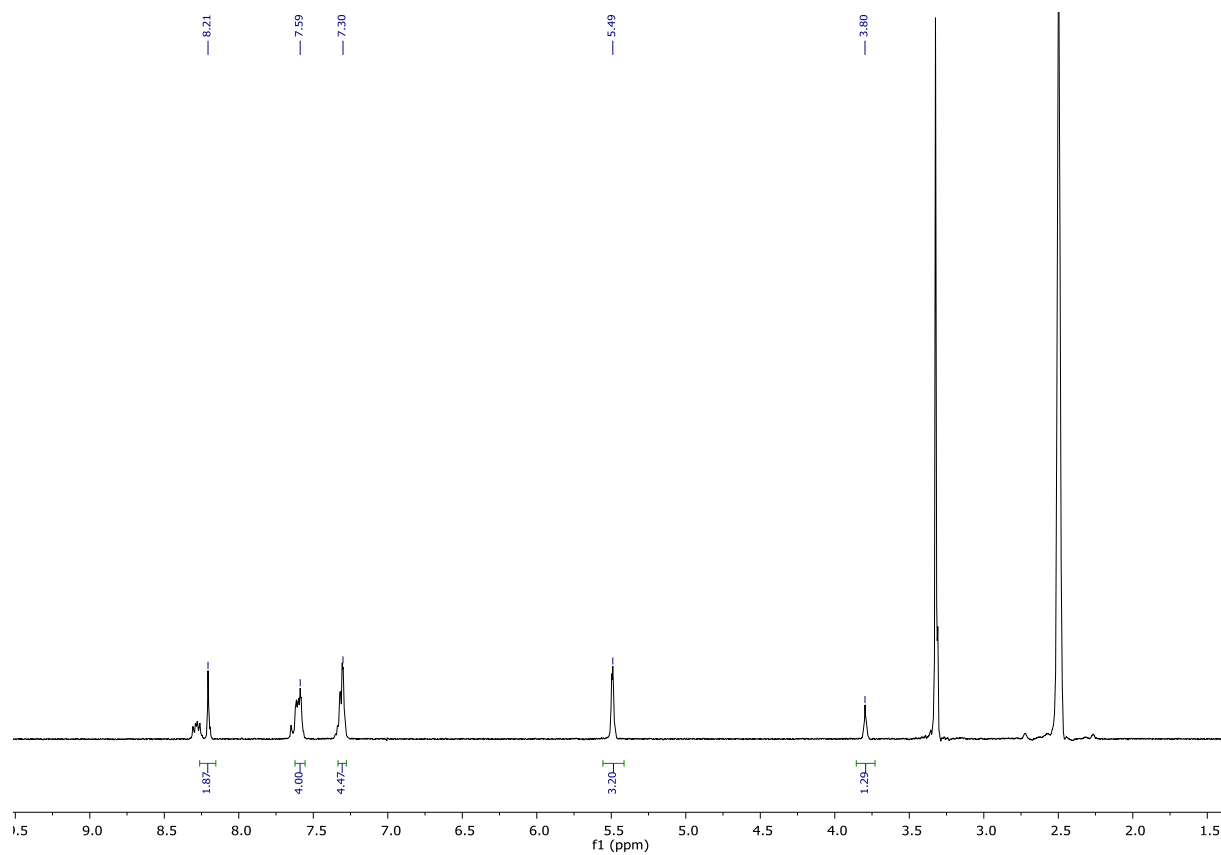


Figure S20. ^1H -NMR ($\text{DMSO-}d_6$) of 2-((4-Fluorophenyl)diazenyl)- 1,3-bis-(propargyl)-1H-imidazolium hexafluorophosphate(6)

1,3-Bis(2-((4-fluorophenyl)diazenyl)-1H-imidazol-1-yl)propan-2-ol (7)

$^1\text{H NMR}$ (300 MHz, $\text{DMSO-}d_6$) $\delta = 8.02 - 7.08$ (m, 12H), 5.75 (s, 1H), 4.73 - 4.09 (m, 5H) ppm.

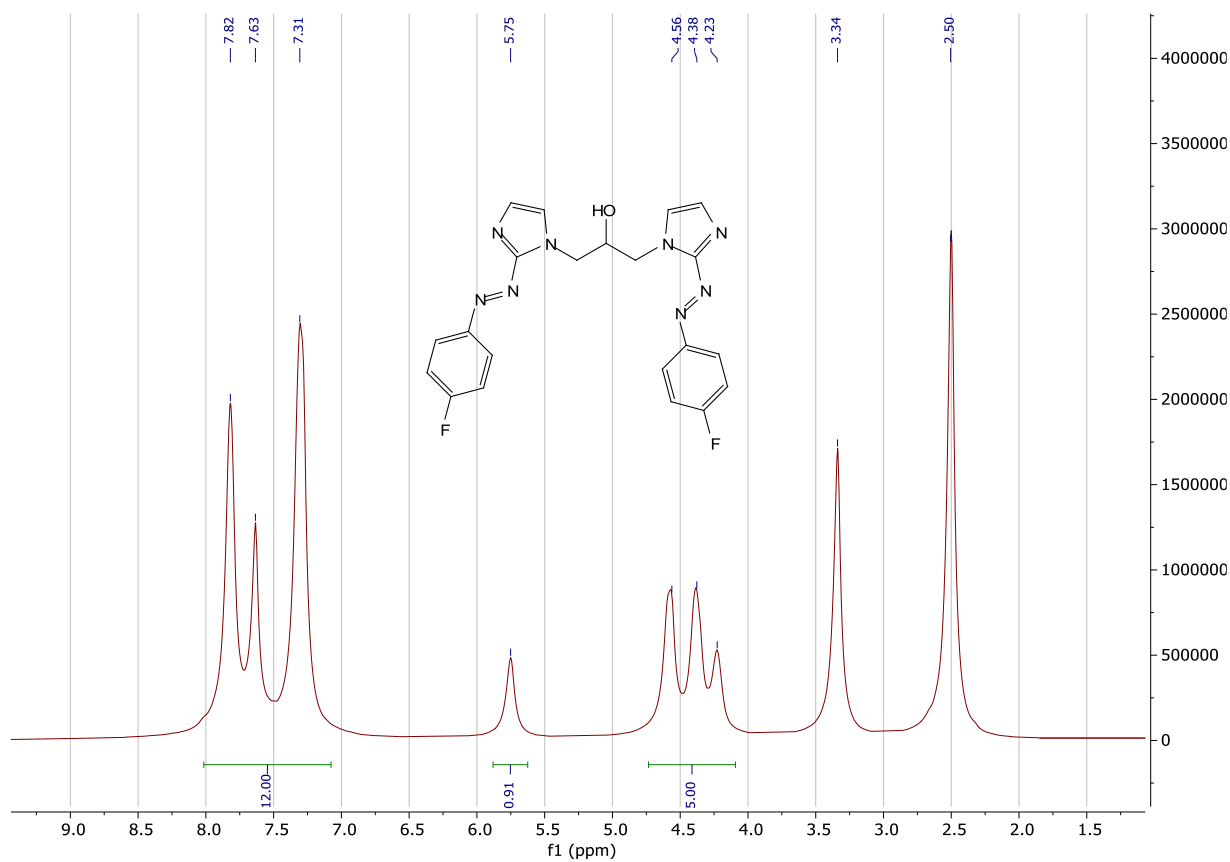


Figure S21. $^1\text{H-NMR}$ ($\text{DMSO-}d_6$) of 1,3-Bis(2-((4-fluorophenyl)diazenyl)-1H-imidazol-1-yl)propan-2-ol (7)

IR(neat): $\nu = 3537$ (w), 3359 (w), 3261 (w), 3103 (w), 2938 (w), 2864 (w), 2780 (w), 2556 (w), 2449 (w), 2343 (w), 1715 (w), 1590 (m), 1498 (m), 1498 (m), 1362 (m), 1291 (m), 1226(s), 1130 (w), 1092 (m), 1036 (w), 955 (w), 845 (s), 778 (m) cm^{-1} .

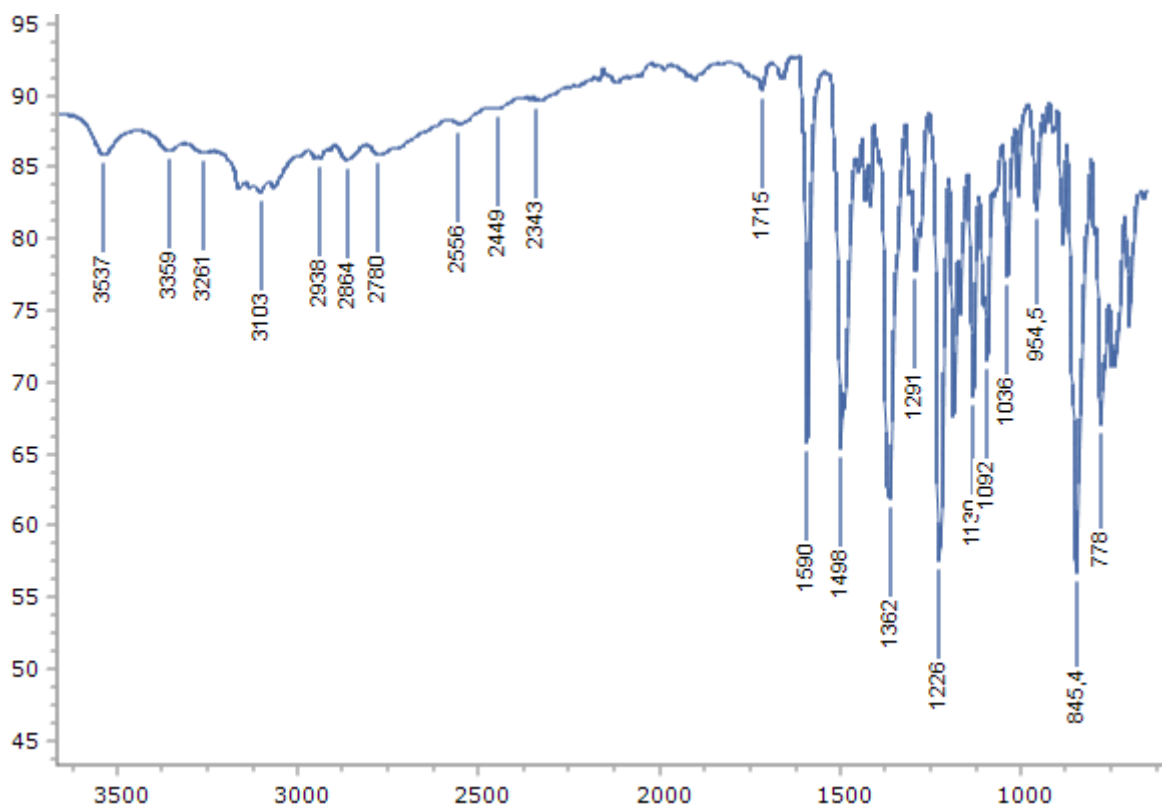


Figure S22. IR- absorption spectra (neat) of 1,3-Bis(2-((4-fluorophenyl)diazenyl)-1H-imidazol-1-yl)propan-2-ol (**7**)

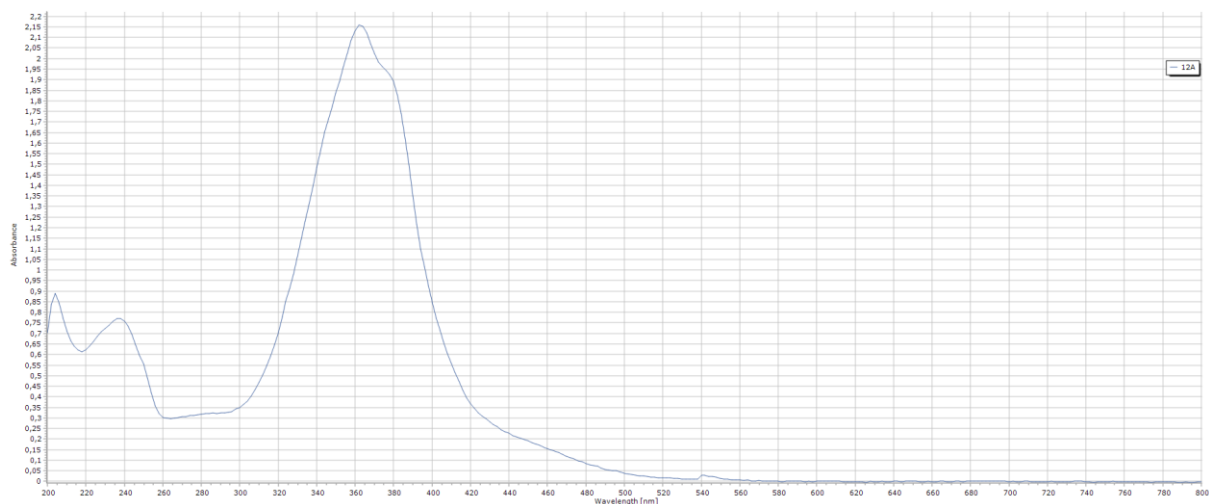


Figure S23. UV/Vis spectra (neat) of 1,3-Bis(2-((4-fluorophenyl)diazenyl)-1H-imidazol-1-yl)propan-2-ol (**7**)

Hot stage microscopy – contact preparation of compound (5)

Contact preparations of **5** with $\text{Bu}_4\text{N}^+\text{N}_3^-$ and KSCN were produced by melting a suitable amount **5** between a glass slide and a cover slip using a Kofler hot bench. After cooling the melt, a crystalline film of **5** is formed occupying about the halve of the space between the glass slide and the cover slip. A small amount of the reactants (tetrabutylammonium azide and potassium thiocyanate, respectively) were placed at the edge of the cover slip (at the opposite site of the resolidified melt of **5**) and then selectively melted at the hot bench to fill the remaining empty space below the cover slip. As soon as the melt gets in contact with the crystalline film of **5**, the preparation was quickly removed from the hot surface, quench cooled on a cold metal block, transferred to the hot stage microscope. Observations were performed on reheating such preparations.



.avi
IMG_4156.avi

Figure S24. Movie showing resolidified melt of dichroitic 2-(4-fluorophenyl)diazenyl)-1,3-diethylimidazolium tetrafluoroborate (**5**) in contact with the ionic liquid tetrabutylammonium azide (M.p. 89 °C) expelling nitrogen bubbles under formation of a deep purple secondary dye.

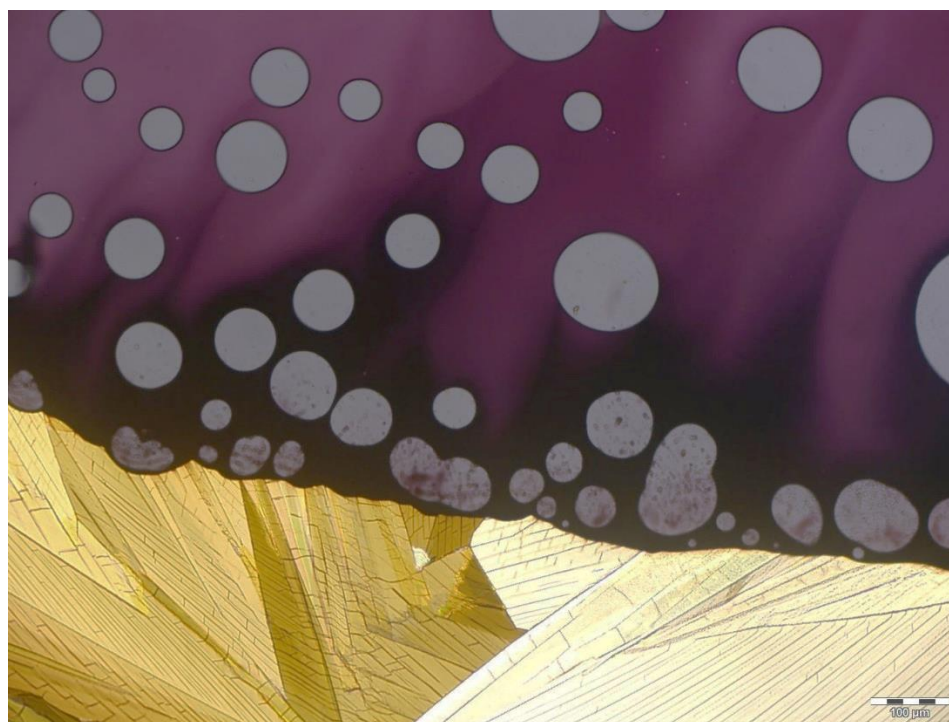


Figure S25. Resolidified melt of dichroitic 2-(4-fluorophenyl)diazenyl)-1,3-diethylimidazolium tetrafluoroborate (**5**) in contact with the ionic liquid tetrabutylammonium azide (M.p. 89 °C) expelling nitrogen bubbles under formation of a deep purple secondary dye. The purple dye is soluble in the liquid of $\text{Bu}_4\text{N}^+\text{N}_3^-$ and is staining the bulk liquid.

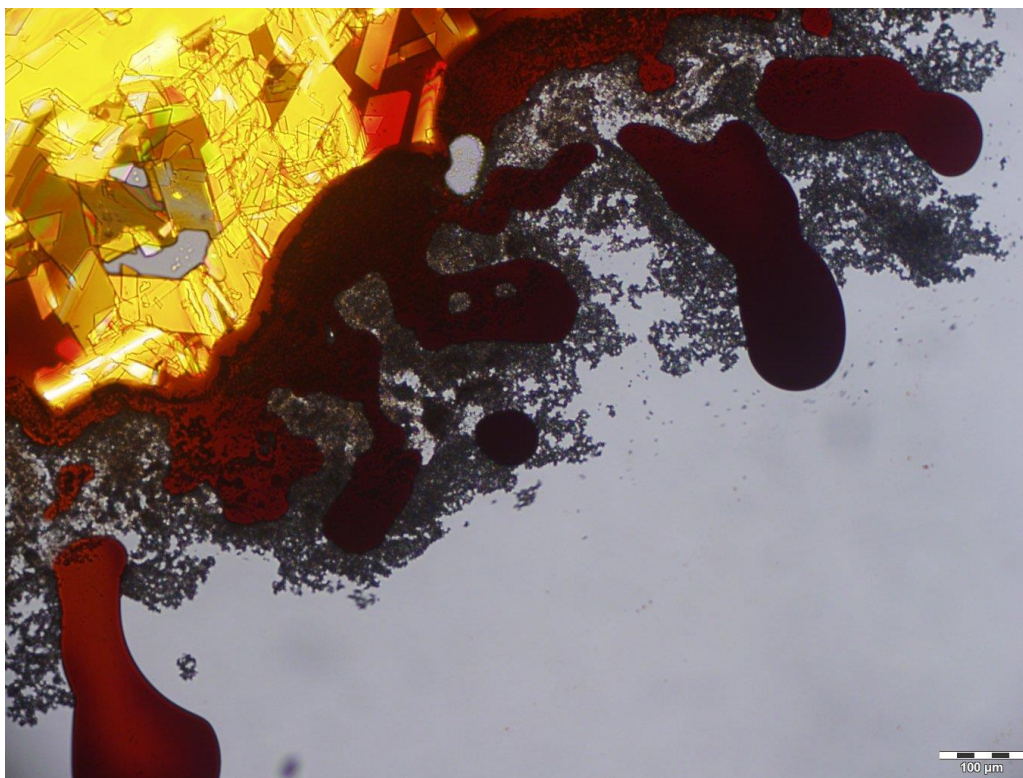


Figure S26. Resolidified melt of dichroic 2-(4-fluorophenyl)diazenyl)-1,3-diethylimidazolium tetrafluoroborate (**5**) in contact with molten KSCN (M.p. 175 °C) forming a deep purple secondary dye and a greyish precipitate (supposedly KBF_4).

Dichroism of 2-(4-fluorophenyl)diazenyl)-1,3-diethylimidazolium tetrafluoroborate (5)

Figure S27 shows a microscopic oil preparation of 2-(4-fluorophenyl)diazenyl)-1,3-diethylimidazolium tetrafluoroborate (5) recorded at different rotation angles in linear polarized light, confirming the dichroitic behavior.

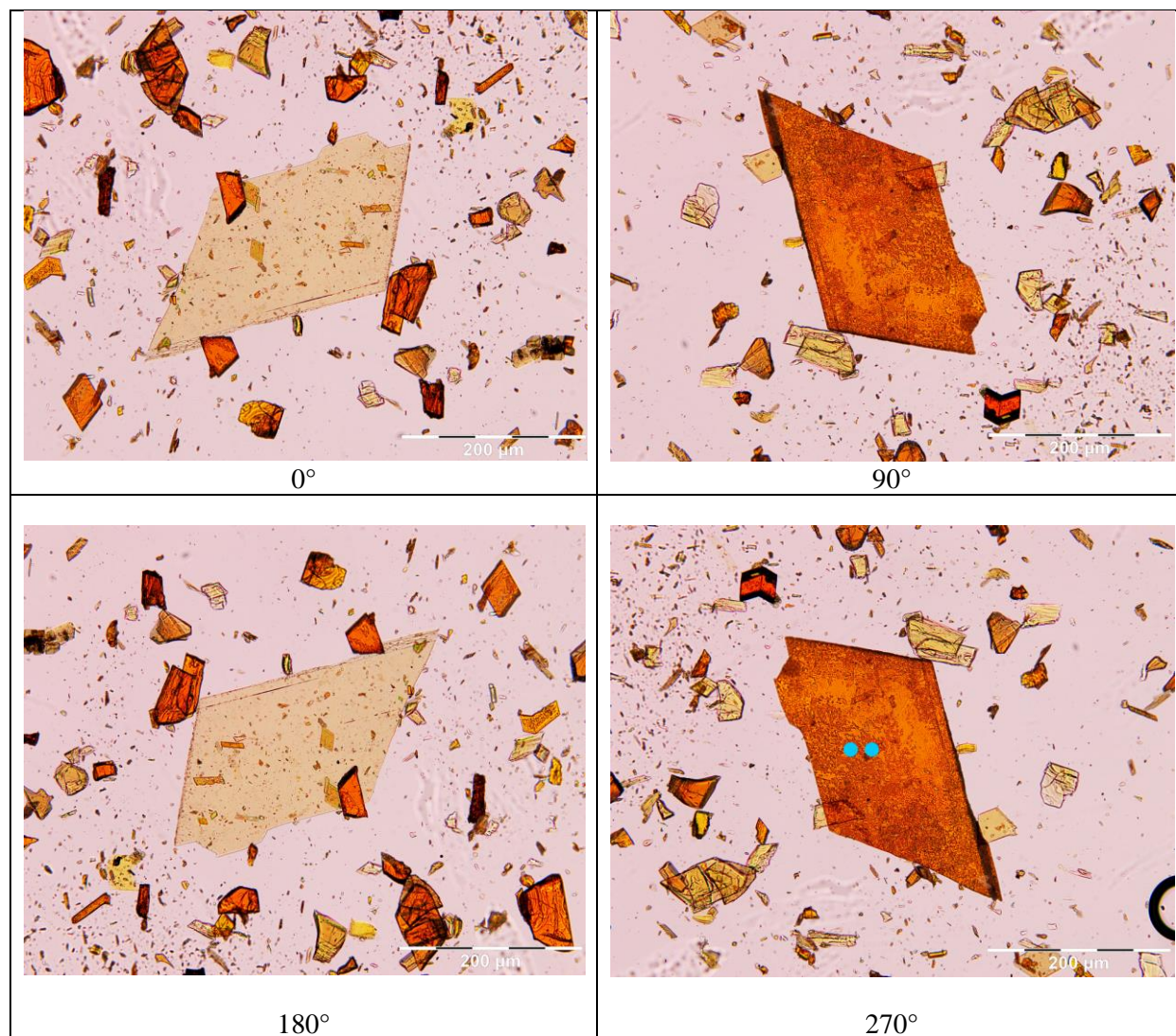


Figure S27. Photomicrographs showing the dichroism of a single crystal (center) of 2-(4-fluorophenyl)diazenyl)-1,3-diethylimidazolium tetrafluoroborate (5) under linear polarized light at the relative rotation angles of 0, 90, 180 and 270 °.